

The \mathcal{PT} -symmetric quantum Rabi model: Solutions and exceptional points

Jiong Li and Yi-Cheng Wang

School of Physics, Zhejiang University, Hangzhou 310027, China

Li-Wei Duan*

Department of Physics, Zhejiang Normal University, Jinhua 321004, China

Qing-Hu Chen†

School of Physics, Zhejiang University, Hangzhou 310027, China and

Collaborative Innovation Center of Advanced Microstructures, Nanjing University, Nanjing 210093, China

(Dated: March 26, 2024)

The non-Hermitian one-photon and two-photon quantum Rabi models (QRMs) with imaginary couplings are respectively solved through the Bogoliubov operators approach. Transcendental functions responsible for exact solutions are derived, whose zeros produce the complete spectra. Exceptional points (EPs) can be identified in terms of the transcendental function. The EP is formed in the two nearest-neighboring excited energy levels, and shifts towards lower coupling strength at higher energy levels. Interestingly, under the resonant condition in the non-Hermitian two-photon QRM, the lowest two excited states within the same parity in the even photonic number subspace coalesce at an EP, but take always the purely real energy, in sharp contrast to the conventional EP in the non-Hermitian systems. For both non-Hermitian QRMs, the fidelity susceptibility goes to negative infinity at the EPs, consistent with the recent observations in non-Hermitian systems. All eigenstates can be labeled by the conserved energy and the QRM parity, we argue that the non-Hermitian QRMs are also integrable, similar to their Hermitian counterparts.

Keywords: non-Hermitian quantum Rabi models, the Bogoliubov operators approach, exceptional points

I. INTRODUCTION

The non-Hermitian systems have attracted considerable interest in recent years. Different from the Hermitian case, the non-Hermitian systems involve energy exchange with the environment, leading to Hamiltonians that typically yield complex spectra. Non-Hermitian Hamiltonians arise in a variety of physical areas, including cold atoms systems, superconductor vortex pinning, and surface hopping [1–6]. Many theoretical approaches have been proposed to explore their unusual properties, such as the Feshbach projection, biorthogonal quantum mechanics, and nonunitary conformal field theory in the literature [7–11].

Remarkably, under specific conditions, the non-Hermitian Hamiltonian with parity-time (\mathcal{PT}) symmetry can maintain entirely real eigenvalue spectra [12–15]. For a \mathcal{PT} -symmetric Hamiltonian H with $H|\phi\rangle = E|\phi\rangle$, the parity-time operator \mathcal{PT} satisfies $\mathcal{PT}H\mathcal{PT} = H$, resulting in $\mathcal{PT}H|\phi\rangle = H\mathcal{PT}|\phi\rangle = E^*\mathcal{PT}|\phi\rangle$. Consequently, the spectra are either complex-conjugate or entirely real when \mathcal{PT} symmetry is maintained. The concept of \mathcal{PT} symmetry has been successfully employed in controlled dissipation, trapped ions, superconductivity [16–20]. Exceptional points (EPs), marking the transition between the symmetric and broken phases, signal the transition of eigenvalues to become complex, leading to unexpected

features such as band-merging, unidirectional invisibility, and fast self-pulsations [21–23].

The quantum Rabi model (QRM) is the simplest model describing the light-matter interaction between a two-level system and a single-mode cavity [24]. It has wide applications in various physical fields, such as the cavity and circuit quantum electrodynamics (QED) systems, solid state semiconductor systems, trapped ions, and quantum dots. The two-level system in the QRM serves as a building-block qubit for realizing quantum simulations and computations [25–32]. Furthermore, its nonlinear atom-cavity coupling variants are utilized to describe physical phenomena in recent experiments or quantum simulations involving multi-photon scenarios. As an example, the two-photon quantum Rabi model (tpQRM) has been proposed to induce a biexciton quantum dot via a coherent two-photon process, exhibiting spectral collapse [33–38].

The analytical exact solution for the QRM remained elusive until Braak presented a transcendental function, termed as the G -function, using the Bargmann space representation [39]. Quickly, this G -function was reproduced using the Bogoliubov operator approach (BOA) in a more physical way [40], while the G -function of the two-photon QRM was also derived. The two-photon G -function exhibits notable features, including the spectral collapse [36, 41–44]. Very interestingly, Braak reproduced this two-photon G -function in the Bargmann space [45] recently, and found that only the two-photon G -function by Chen et al., [40] exhibits an explicitly known pole structure which dictates the collapse point.

The non-Hermitian semi-classical Rabi model with \mathcal{PT}

* duanlw@zjnu.edu.cn

† qhchen@zju.edu.cn

symmetry has been recently studied. Lee set the coupling constant purely imaginary and found gain and loss in time of the two-level systems [46]. Exact Floquet solutions exist for certain EPs in a time-periodic \mathcal{PT} -symmetric Rabi model under the condition of multiple-photon resonances [47]. The fully quantized Rabi model (QRM) could also possess \mathcal{PT} symmetry and hold potential applications for the open quantum system. For the purely imaginary bias in the QRM [48], multiple EPs appear with increasing light-matter coupling strength, contrary to the only single EP in the whole phase diagram of most non-Hermitian systems.

In this work, we extend the non-Hermitian semi-classical Rabi model to a fully quantized version, and explore the non-Hermitian one-photon and two-photon QRMs with imaginary coupling constants. The paper is structured as follows: In Sec. II, the previous G -function technique is generalized to the non-Hermitian QRM, and the exact energy spectra as well as the EPs are obtained analytically by the derived G -function. Similar studies are carried out for the non-Hermitian tpQRM in Sec. III. A new kind of EP is observed in the resonate case for the tpQRM. We summarize our findings and discussions in Sec. IV.

II. NON-HERMITIAN QUANTUM RABI MODEL

The Hamiltonian of the non-Hermitian QRM is expressed as

$$H = -\frac{\Delta}{2}\sigma_x + \omega a^\dagger a + ig(a + a^\dagger)\sigma_z, \quad (1)$$

where a , a^\dagger are photon annihilation and creation operators of the single-mode cavity with frequency ω , ig is the purely imaginary qubit-cavity coupling constant, Δ is the tunneling matrix element, and $\sigma_{x,y,z}$ are the Pauli matrices. For simplicity, ω is set 1 throughout this paper.

We define a parity operator

$$\mathcal{P} = \sigma_x \otimes \mathbb{1},$$

where $\mathbb{1}$ is the identity operator for the single-mode cavity. Note that it is different from the corresponding QRM operator $\Pi_{1p} = \sigma_x \otimes \exp[i\pi a^\dagger a]$ in the Hermitian case. The usual time-reversal operator \mathcal{T} takes the complex conjugate, thus $\mathcal{T}\hat{x}\mathcal{T} = \hat{x}$, $\mathcal{T}\hat{p}\mathcal{T} = -\hat{p}$, where \hat{x} is the displacement operator and \hat{p} is the momentum operator, yielding $\mathcal{T}a(a^\dagger)\mathcal{T} = a(a^\dagger)$. We therefore have

$$\begin{aligned} \mathcal{P}\mathcal{T}H\mathcal{T}\mathcal{P} &= \mathcal{P}\left(a^\dagger a - ig(a + a^\dagger)\sigma_z - \frac{\Delta}{2}\sigma_x\right)\mathcal{P} \\ &= a^\dagger a + ig(a + a^\dagger)\sigma_z - \frac{\Delta}{2}\sigma_x = H, \end{aligned} \quad (2)$$

demonstrating this Hamiltonian is indeed \mathcal{PT} -symmetric.

A. Solutions within Bogoliubov transformation

Different from the unitary transformation in [40], we employ a similar transformation $D(ig) = e^{ig(a^\dagger - a)}$ that satisfies

$$\begin{aligned} D(ig)aD(-ig) &= a - ig, D(ig)a^\dagger D(-ig) = a^\dagger - ig \\ D(ig)D(-ig) &= 1, D(ig)^\dagger D(ig) = D(2ig) \neq 1. \end{aligned} \quad (3)$$

Then the Hamiltonian Eq. (1) is reformed by two opposite transformations

$$\begin{aligned} H_+ &= D(ig)HD(-ig) \\ &= \begin{bmatrix} a^\dagger a + g^2 & -\frac{\Delta}{2} \\ -\frac{\Delta}{2} & a^\dagger a - 2ig(a + a^\dagger) - 3g^2 \end{bmatrix}, \end{aligned} \quad (4a)$$

$$\begin{aligned} H_- &= D(-ig)HD(ig) \\ &= \begin{bmatrix} a^\dagger a + 2ig(a + a^\dagger) - 3g^2 & -\frac{\Delta}{2} \\ -\frac{\Delta}{2} & a^\dagger a + g^2 \end{bmatrix}. \end{aligned} \quad (4b)$$

The general expansion of eigenfunction for H_+ is proposed as

$$|+\rangle = \left[\frac{\sum_{n=0}^{+\infty} i^{-n} \sqrt{n!} e_n |n\rangle}{\sum_{n=0}^{+\infty} i^{-n} \sqrt{n!} f_n |n\rangle} \right],$$

where e_n and f_n are the expansion coefficients, and $\{|n\rangle\}$ are Fock states generated by a^\dagger acting on the photon vacuum state. Subsequently, a recursive relation of e_n and f_n is formulated by the Schrödinger equation $H_+|+\rangle = E|+\rangle$ and projection onto $|n\rangle$,

$$e_n = \frac{\frac{\Delta}{2} f_n}{n + g^2 - E}, \quad (5a)$$

$$f_{n+1} = \frac{-\frac{\Delta}{2} e_n + (n - 3g^2 - E) f_n}{2g(n+1)} + \frac{f_{n-1}}{n+1}. \quad (5b)$$

Similarly, set the general expansion of eigenfunction for H_- as

$$|-\rangle = \left[\frac{\sum_{n=0}^{+\infty} i^{-n} \sqrt{n!} c_n |n\rangle}{\sum_{n=0}^{+\infty} i^{-n} \sqrt{n!} d_n |n\rangle} \right],$$

and the recursive relation of c_n and d_n is determined by the same procedure,

$$d_n = \frac{\frac{\Delta}{2} c_n}{n + g^2 - E}, \quad (6a)$$

$$c_{n+1} = \frac{\frac{\Delta}{2} d_n - (n - 3g^2 - E) c_n}{2g(n+1)} + \frac{c_{n-1}}{n+1}. \quad (6b)$$

Comparing Eq. (6) with (5), the eigenfunction for H_- can be expressed as

$$|-\rangle = \left[\frac{\sum_{n=0}^{+\infty} (-i)^{-n} \sqrt{n!} f_n |n\rangle}{\sum_{n=0}^{+\infty} (-i)^{-n} \sqrt{n!} e_n |n\rangle} \right]. \quad (7)$$

Transforming back to the original Hamiltonian, we have

$$|\Psi\rangle_+ = D(-ig)|+\rangle, |\Psi\rangle_- = D(ig)|-\rangle. \quad (8)$$

These two eigenfunctions should describe the same eigenstate, i.e. $|\Psi\rangle_+ \propto |\Psi\rangle_-$. Projecting onto the photon vacuum state $|0\rangle$, we finally get the G -function

$$\begin{bmatrix} \sum_{n=0}^{+\infty} e_n g^n \\ \sum_{n=0}^{+\infty} f_n g^n \end{bmatrix} \propto \begin{bmatrix} \sum_{n=0}^{+\infty} f_n g^n \\ \sum_{n=0}^{+\infty} e_n g^n \end{bmatrix}, \quad (9)$$

$$G_{\pm} = \sum_{n=0}^{+\infty} (e_n \mp f_n) g^n = 0, \quad (10)$$

whose zeros correspond to energy eigenvalues. All f_n and e_n can be determined through Eq. (5) and $f_0 = 1$. By the way, Eq. (5a) yields the pole structure

$$E_n^{(pole)} = n + g^2. \quad (11)$$

The G -function in (10) is currently in the form of the real number. In practice, we can get some real zeros, namely real eigenvalues, as shown in the upper panel of Fig. 1. Nevertheless, in the high- E regime, the real zero does not exist. In this case, the zeros of the G -function (i.e., $Re(G) = Im(G) = 0$) can give rise to the complex eigenenergies. Both the real and complex zeros of the G -function are marked with open circles in the lower panel of Fig. 1.

For a pair of complex-conjugate eigenenergies E and E^* , from Eqs. (5a) and (5b) we find $e_n(E^*) = e_n^*(E)$ and $f_n(E^*) = f_n^*(E)$, resulting in $G_{\pm}(E^*) = G_{\pm}^*(E)$. Therefore, if E is a solution of $G_+ = 0$ ($G_- = 0$), E^* must also be a solution of $G_+ = 0$ ($G_- = 0$). As shown in the lower panel of Fig. 1, the complex zeros of G -function are located symmetrically with $Im(E) = 0$ line, indicating complex-conjugate eigenenergies.

B. Exceptional Points and Symmetry

Fig. 2 presents the energy spectra with both the real and imaginary parts for $\Delta = 0.50$. The results by the numerical exact diagonalization are the same as those by the zeros of the G -function. The EPs are located at the points where the two real energies begin to merge into a single one and the imaginary energy just appears.

It is worth noting that the parity $\Pi_{1p} = \sigma_x \otimes e^{i\pi a^\dagger a}$ for the QRM still holds for the non-Hermitian QRM. \pm in the G -function (10) just stand for the positive and negative parity, respectively, similar to the Hermitian case [40]. As discussed above, a pair of complex-conjugate levels are simultaneously determined by the zeros of either G_+ or G_- , thus possess the same parity.

An EP means that the G -function has only one zero between two adjacent poles. As shown in Fig. 3, the EP can be obtained when both the G -function and its

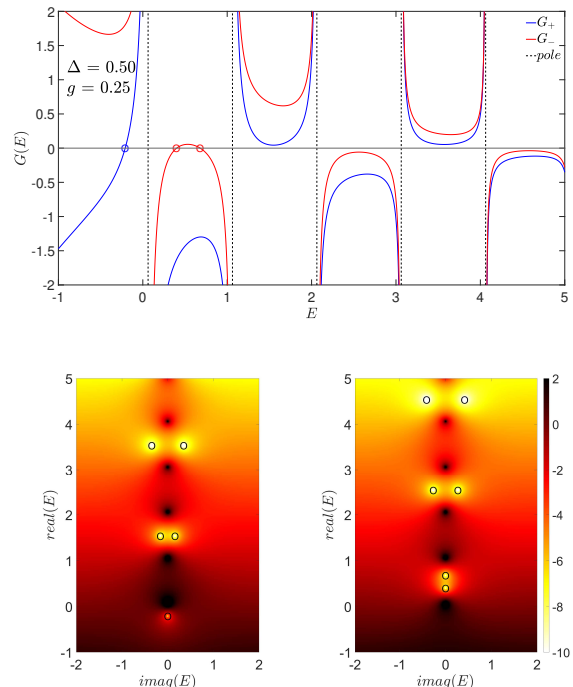


FIG. 1: (colored online) The upper panel presents G -curves in the real E regime. The blue (red) lines marks G_+ (G_-) curves, the black dashed lines denote $E_n^{(pole)}$. The lower panel gives $\ln|G_+|^2$ (left) and $\ln|G_-|^2$ (right) in the complex energy plane, respectively. The opened circles are just the zeros. $\Delta = 0.50$ and $g = 0.25$.

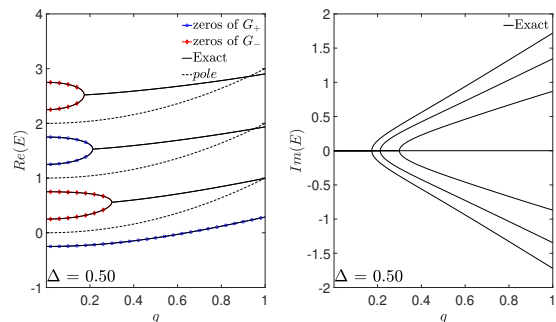


FIG. 2: (colored online) The real part (left) and imaginary part (right) of the energy levels as a function of the coupling strength g for $\Delta = 0.50$. The black solid lines are eigenenergies obtained by the exact diagonalization (ED), and the dashed lines are $E_n^{(pole)}$. The blue lines with circles are zeros of G_+ , and the red lines with diamonds are zeros of G_- .

first-order derivative with respect to energy, $\partial G_{\pm}/\partial E$, are zero simultaneously.

Now the eigenfunction can be expressed as

$$|\Psi\rangle = \begin{bmatrix} \sum_{n=0}^{+\infty} i^{-n} \sqrt{n!} e_n D(-ig)|n\rangle \\ \pm \sum_{n=0}^{+\infty} (-i)^{-n} \sqrt{n!} e_n D(ig)|n\rangle \end{bmatrix}, \quad (12)$$

where \pm correspond to eigenvalues ± 1 of Π_{1p} . The \mathcal{PT}

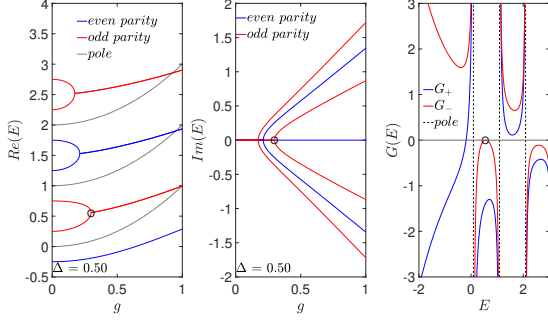


FIG. 3: (colored online) The left (middle) panel presents the real (imaginary) energy levels as a function of the coupling strength g . The right panel gives the G -curves at the same g as that of the first EP indicated by open circles in the left and middle panels. The blue (red) lines mark even (odd) Π_{1p} parity levels. The dashed lines denote $E_n^{(pole)}$. The blue (red) lines in the right panel mark G_+ (G_-), respectively. $\Delta = 0.50$.

operator acts on $|\Psi\rangle$,

$$\begin{aligned} \mathcal{PT}|\Psi\rangle &= (\sigma_x \otimes \mathbb{1})\mathcal{T} \left[\begin{array}{l} \sum_{n=0}^{+\infty} i^{-n} \sqrt{n!} e_n D(-ig)|n\rangle \\ \pm \sum_{n=0}^{+\infty} (-i)^{-n} \sqrt{n!} e_n D(ig)|n\rangle \end{array} \right] \\ &= \left[\pm \sum_{n=0}^{+\infty} i^{-n} \sqrt{n!} e_n^* D(-ig)|n\rangle \right]. \end{aligned} \quad (13)$$

Before the EP, all e_n are real, hence $\mathcal{PT}|\Psi\rangle$ is simply $\pm|\Psi\rangle$, indicating the preservation of \mathcal{PT} symmetry. After the EP, \mathcal{PT} symmetry is broken, and $\{e_n^*\}$ for E correspond to $\{e_n\}$ for E^* , leading to the \mathcal{PT} operator transforming $|\Psi\rangle$ into its conjugate counterpart.

Now we can explain why two eigenvalues and eigenvectors coalesce at EPs in this model. Since at an EP, the two energies become the same from the single G -function, thus the eigenstates are also the same $|\Psi\rangle$, with the same coefficients e_n, f_n . Note that in the Juddian solution of the Hermitian QRM, the doubly degenerate states cannot be obtained from the zero of G -function, at the crossing points, there are actually two different states [39].

The EPs can also be examined by calculating fidelity susceptibility

$$\chi = \frac{1 - \langle L(\lambda)|R(\lambda + \epsilon)\rangle \langle L(\lambda + \epsilon)|R(\lambda)\rangle}{\epsilon^2}, \quad (14)$$

where $|L\rangle$ and $|R\rangle$ are bra and ket of biorthogonal basis respectively [10]. The limit of $Re(\chi(g))$ tends to negative infinity when g approaches an EP, as illustrated in Fig. 4. Note that in the practical calculations, the truncation number of the summation in the G -function given by Eq. (10) cannot be really infinite, so the $Re(\chi(g))$ is only extremely negatively large.

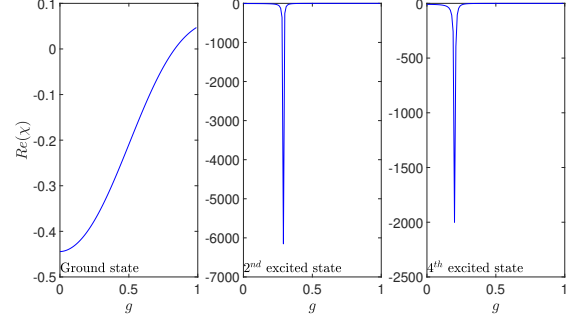


FIG. 4: Fidelity susceptibility as a function of the coupling strength g for the ground state (left panel), the 2^{nd} excited state (middle panel) and the 4^{th} excited state (right panel) at $\Delta = 0.5$.

III. NON-HERMITIAN TWO-PHOTON QUANTUM RABI MODEL

Next, we turn to the non-Hermitian tpQRM described by the following Hamiltonian

$$H_{2pNH} = -\frac{\Delta}{2}\sigma_x + a^\dagger a + ig(a^2 + (a^\dagger)^2)\sigma_z, \quad (15)$$

which is a natural extension of the non-Hermitian QRM.

The parity operator $\mathcal{P} = \sigma_x \otimes \mathbb{1}$ and the time-reversal operator \mathcal{T} defined previously still satisfy

$$\begin{aligned} \mathcal{PT}H_{2pNH}\mathcal{TP} &= \mathcal{P} \left(a^\dagger a - ig(a^2 + (a^\dagger)^2)\sigma_z - \frac{\Delta}{2}\sigma_x \right) \mathcal{P} \\ &= a^\dagger a + ig(a^2 + (a^\dagger)^2)\sigma_z - \frac{\Delta}{2}\sigma_x = H. \end{aligned}$$

Therefore, this Hamiltonian is also \mathcal{PT} -symmetric.

A. Solutions within Bogoliubov transformation

The G -function for non-Hermitian tpQRM can be derived in a similar way as for tpQRM [41]. Analogously, a similar transformation

$$S(ir) = e^{i\frac{\pi}{2}((a^\dagger)^2 - a^2)},$$

where

$$r = \frac{1}{2} \cos^{-1} \frac{1}{\beta}, \beta = \sqrt{1 + 4g^2}, \quad (16)$$

is introduced, thus we have

$$\begin{aligned} S(ir)aS(-ir) &= a \cos r - ia^\dagger \sin r, \\ S(ir)a^\dagger S(-ir) &= a^\dagger \cos r - ia \sin r, \\ S(ir)S(-ir) &= 1, \quad S(ir)^\dagger S(ir) = S(2ir) \neq 1. \end{aligned} \quad (17)$$

Hamiltonian (15) is then reformed by two opposite transformation

$$\begin{aligned} H_+^{2p} &= S(ir)H_{2pNH}S(-ir) = \\ &= \left[\begin{array}{c} \beta \left(a^\dagger a + \frac{1}{2} \right) - \frac{1}{2} \quad -\frac{\Delta}{2} \\ -\frac{\Delta}{2} \quad \frac{(2-\beta^2)(a^\dagger a + \frac{1}{2}) - 2ig(a^2 + (a^\dagger)^2)}{\beta} - \frac{1}{2} \end{array} \right], \end{aligned}$$

$$H_-^{2p} = S(-ir)H_{2pNH}S(ir) = \begin{bmatrix} \frac{(2-\beta^2)(a^\dagger a + \frac{1}{2}) + 2ig(a^2 + (a^\dagger)^2)}{\beta} - \frac{1}{2} & -\frac{\Delta}{2} \\ -\frac{\Delta}{2} & \beta(a^\dagger a + \frac{1}{2}) - \frac{1}{2} \end{bmatrix}.$$

Next, we define a set of ladder operators which satisfy su(1,1) Lie algebra,

$$K_0 = \frac{1}{2} \left(a^\dagger a + \frac{1}{2} \right), \quad K_+ = \frac{1}{2} (a^\dagger)^2, \quad K_- = \frac{1}{2} a^2, \quad (19)$$

where

$$[K_0, K_\pm] = \pm K_\pm, [K_+, K_-] = -2K_0. \quad (20)$$

The Hilbert space \mathcal{H} generated by a^\dagger acting on the photon vacuum state $|0\rangle$, suppresses into two subspaces characterized by the so-called Bargmann index q : $K_0|q,0\rangle = q|q,0\rangle$. For the even photonic subspace $\mathcal{H}_{\frac{1}{4}} = \{(a^\dagger)^n|0\rangle, n=0,2,4,\dots\}$, $q = \frac{1}{4}$ and for the odd photonic subspace $\mathcal{H}_{\frac{3}{4}} = \{(a^\dagger)^n|0\rangle, n=1,3,5,\dots\}$, $q = \frac{3}{4}$.

$$|q, n\rangle = \left| 2 \left(q + n - \frac{1}{4} \right) \right\rangle = \frac{(a^\dagger)^{2(q+n-\frac{1}{4})}}{\sqrt{[2(q+n-\frac{1}{4})]!}} |0\rangle,$$

$$K_0|q, n\rangle = (q+n)|q, n\rangle,$$

$$K_+|q, n\rangle = \sqrt{\left(n + q + \frac{1}{4} \right) \left(n + q + \frac{3}{4} \right)} |q, n+1\rangle,$$

$$K_-|q, n\rangle = \sqrt{\left(n + q - \frac{1}{4} \right) \left(n + q - \frac{3}{4} \right)} |q, n-1\rangle.$$

In term of K_0, K_\pm , the Hamiltonian H_+^{2p} becomes

$$H_+^{2p} = \begin{bmatrix} 2\beta K_0 - \frac{1}{2} & -\frac{\Delta}{2} \\ -\frac{\Delta}{2} & \frac{2K_0(2-\beta^2) - 4ig(K_+ + K_-)}{\beta} - \frac{1}{2} \end{bmatrix}. \quad (21)$$

Now, we propose the general expansion for the eigenfunction of H_+^{2p} as

$$|+^{(q)}\rangle = \left[\frac{\sum_{n=0}^{+\infty} \sqrt{[2(n+q-\frac{1}{4})]!} i^n e_n^{(q)} |q, n\rangle}{\sum_{n=0}^{+\infty} \sqrt{[2(n+q-\frac{1}{4})]!} i^n f_n^{(q)} |q, n\rangle} \right], \quad (22)$$

where $e_n^{(q)}$ and $f_n^{(q)}$ are the expansion coefficients. By the Schrödinger equation $H_+ |+^{(q)}\rangle = E |+^{(q)}\rangle$ and projecting onto $|q, n\rangle$, a recursive relation of $e_n^{(q)}$ and $f_n^{(q)}$ is derived as

$$e_n^{(q)} = \frac{\frac{\Delta}{2} f_n^{(q)}}{2(n+q)\beta - \frac{1}{2} - E}, \quad (23a)$$

$$f_{n+1}^{(q)} = \frac{[2(n+q)(2-\beta^2) - \beta(\frac{1}{2} + E)] f_n^{(q)}}{4g(n+q+\frac{1}{4})(n+q+\frac{3}{4})} + \frac{4g f_{n-1}^{(q)} - \frac{\Delta}{2} \beta e_n^{(q)}}{4g(n+q+\frac{1}{4})(n+q+\frac{3}{4})}. \quad (23b)$$

Similarly, the general expansion for the eigenfunction of H_- can be expressed as

$$|-^{(q)}\rangle = \left[\frac{\sum_{n=0}^{+\infty} \sqrt{[2(n+q-\frac{1}{4})]!} (-i)^n f_n^{(q)} |q, n\rangle}{\sum_{n=0}^{+\infty} \sqrt{[2(n+q-\frac{1}{4})]!} (-i)^n e_n^{(q)} |q, n\rangle} \right]. \quad (24)$$

Transforming back to the original Hamiltonian, we have

$$|\Psi^{(q)}\rangle_+ = S(-ir)|+^{(q)}\rangle, \quad |\Psi^{(q)}\rangle_- = S(ir)|-^{(q)}\rangle. \quad (25)$$

These eigenfunctions should describe the same eigenstate, i.e. $|\Psi^{(q)}\rangle_+ \propto |\Psi^{(q)}\rangle_-$. Projecting onto the the corresponding vacuum state $|q, 0\rangle$, we have

$$\langle q, 0|S(ir)|q, n\rangle \propto \frac{\sqrt{[2(n+q-\frac{1}{4})]!}}{n!} \left(\frac{i \tan r}{2} \right)^n \quad (26)$$

$$\begin{aligned} & \left[\frac{\sum_{n=0}^{+\infty} e_n^{(q)} \frac{[2(n+q-\frac{1}{4})]!}{n!} \left(\frac{\tan r}{2} \right)^n}{\sum_{n=0}^{+\infty} f_n^{(q)} \frac{[2(n+q-\frac{1}{4})]!}{n!} \left(\frac{\tan r}{2} \right)^n} \right] \\ & \propto \left[\frac{\sum_{n=0}^{+\infty} f_n^{(q)} \frac{[2(n+q-\frac{1}{4})]!}{n!} \left(\frac{\tan r}{2} \right)^n}{\sum_{n=0}^{+\infty} e_n^{(q)} \frac{[2(n+q-\frac{1}{4})]!}{n!} \left(\frac{\tan r}{2} \right)^n} \right]. \end{aligned}$$

The G -function is finally formulated as

$$G_\pm^{(q)} = \sum_{n=0}^{+\infty} \left(e_n^{(q)} \mp f_n^{(q)} \right) \frac{[2(n+q-\frac{1}{4})]!}{n!} \left(\frac{\tan r}{2} \right)^n,$$

all $e_n^{(q)}$ and $f_n^{(q)}$ can be determined by recursive relation Eq. (23) from $e_0^{(q)} = 1$. Zeros of $G_\pm^{(q)}$ will give all eigenenergies of the non-Hermitian tpQRM. According to Eq. (23), the n th pole for $G_\pm^{(q)}$ is

$$E_n^{(q,pole)} = 2(n+q)\beta - \frac{1}{2}, \quad (27)$$

one immediately finds that the spectral collapse in [41] does not happen in the corresponding non-Hermitian case, which can also be exhibited in Fig. 5.

The zeros for the G -function vanish in the high- E regime as detailed in Fig. 6, indicating the presence of complex eigenenergies. Since only E is complex in parameters of the recursive relation Eq. (23), $G_\pm^{(q)}(E^*) = G_\pm^{*(q)}(E)$. Therefore, if E is a solution, both E and E^* are the solutions of either $G_+^{(q)} = 0$ or $G_-^{(q)} = 0$ simultaneously.

B. Exceptional Points and Symmetry

The EPs can be presented with the emergence of complex eigenenergies, while the tpQRM parity $\Pi_{2p} = \sigma_x \otimes e^{i\frac{\pi\alpha^\dagger \alpha}{2}}$ remains unaltered. Similar to the non-Hermitian

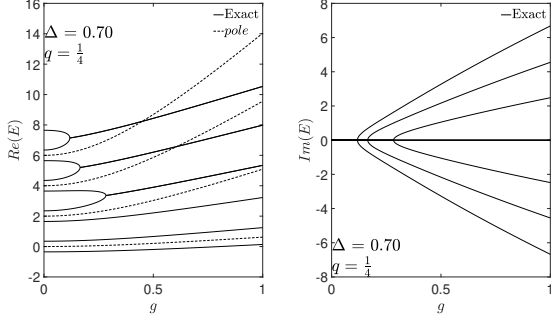


FIG. 5: Real energy levels (left panel) and imaginary energy (right panel) as functions of the coupling strength g for $\Delta = 0.70$ and $q = \frac{1}{4}$ in the tpQRM. The solid lines are eigenenergies obtained by the numerical diagonal method, and the dashed lines are $E_n^{(pole)}$.

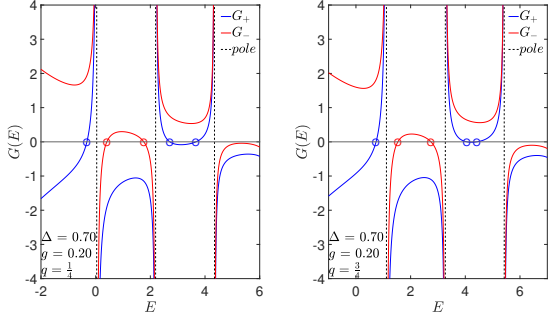


FIG. 6: (colored online) G -curves of the tpQRM for $\Delta = 0.70$, $g = 0.20$ in the real E regime, $q = \frac{1}{4}$ (left panel) and $q = \frac{3}{4}$ (right panel). The blue (red) line mark G_+ (G_-) curves. The black dashed lines denote $E_n^{(q,pole)}$. The opened circles are just the zeros.

QRM, a pair of conjugate levels of non-Hermitian tpQRM also share the same parity with $G_{\pm}^{(q)}(E^*) = G_{\pm}^{(q)*}(E)$.

An EP means that the G -function has only one zero between two adjacent poles. As can be seen in Fig. 7, the EP can still be obtained when both the G -function and its first-order derivative with respect to energy are zero.

Therefore, the eigenfunction can be expressed as

$$|\Psi^{(q)}\rangle = \begin{bmatrix} \sum_{n=0}^{+\infty} \sqrt{[2(n+q-\frac{1}{4})]!} i^n e_n^{(q)} S(-ir) |q, n\rangle \\ \pm \sum_{n=0}^{+\infty} \sqrt{[2(n+q-\frac{1}{4})]!} (-i)^n e_n^{(q)*} S(ir) |q, n\rangle \end{bmatrix}$$

where \pm stands for the even and odd tpQRM parity.

Then the \mathcal{PT} operator acts on the wave function

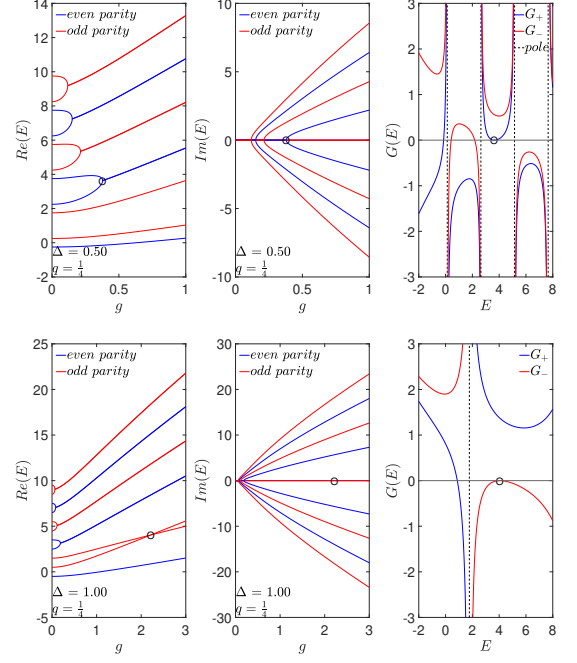


FIG. 7: (colored online) Real energy levels as a function of the coupling strength g (left panel), imaginary energy levels (middle panel), and the G -function (right panel) corresponding to the EP circled in black. The blue (red) lines in the left and the middle panels mark even (odd) Π_{2p} parity levels, respectively. The blue (red) lines in the right panel denote G_+ (G_-), respectively. $\Delta = 0.50$ (upper panel) and $\Delta = 1.00$ (lower panel).

Eq. (28),

$$\begin{aligned} & \mathcal{PT} |\Psi^{(q)}\rangle \\ &= \sigma_x \otimes \mathcal{T} \begin{bmatrix} \sum_{n=0}^{+\infty} \sqrt{[2(n+q-\frac{1}{4})]!} i^n e_n^{(q)} S(-ir) |q, n\rangle \\ \pm \sum_{n=0}^{+\infty} \sqrt{[2(n+q-\frac{1}{4})]!} (-i)^n e_n^{(q)*} S(ir) |q, n\rangle \end{bmatrix} \\ &= \begin{bmatrix} \pm \sum_{n=0}^{+\infty} \sqrt{[2(n+q-\frac{1}{4})]!} i^n e_n^{(q)*} S(-ir) |q, n\rangle \\ \sum_{n=0}^{+\infty} \sqrt{[2(n+q-\frac{1}{4})]!} (-i)^n e_n^{(q)*} S(ir) |q, n\rangle \end{bmatrix}. \end{aligned} \quad (28)$$

In the \mathcal{PT} regime, real energy results in real $e_n^{(q)}$ and $f_n^{(q)}$, leading to $\mathcal{PT} \Psi^{(q)} = \pm |\Psi^{(q)}\rangle$. Meanwhile, in the \mathcal{PT} -broken regime, $\{e_n^{(q)*}\}$ are identical to $\{e_n^{(q)}\}$ corresponding to E^* , analogous to the non-Hermitian QRM. In conclusion, we have proved that the \mathcal{PT} operator transforms the eigenstate to its conjugate counterpart in the \mathcal{PT} -broken regime.

The \mathcal{PT} symmetry can be broken with the emergence of complex eigenenergies at large coupling strength (EP is the critical value), while the original parity $\Pi_{2p} = \sigma_x \otimes e^{i\frac{\pi\sigma_z}{2}}$ of the tpQRM remains unaltered at the same level in the whole coupling regime.

C. Exceptional Point for Real Levels

Precisely at the resonance $\Delta = 1$, it is noteworthy that an EP emerges at the lowest two excited states with real energies, as displayed in Fig. 7. The G -function corresponding to the EP exhibits only one zero, indicating that eigenfunctions for the intersecting real levels are identical at the EP.

Slightly deviation from $\Delta = 1$, say $\Delta = 0.99$ and $\Delta = 1.01$, the EP of real levels disappears, which is clearly shown in Fig. 8. It is surprising that $\Delta = 1$ serves as the only condition for the existence of the exotic real-level EP.

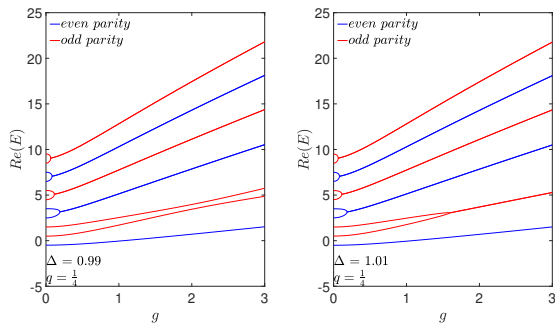


FIG. 8: (colored online) Real energy levels as a function of the coupling strength g for $\Delta = 0.99$ (left panel), and $\Delta = 1.01$ (right panel). The blue (red) lines mark even (odd) Π_{2p} parity levels, respectively.

The real part of $\chi(g)$ of the fidelity susceptibility tends to negative infinity as g approaches EPs, including the real-level EP, as shown in Fig. 9. It is suggested that the real-level crossing point is truly an EP, but may be a new kind of EP.

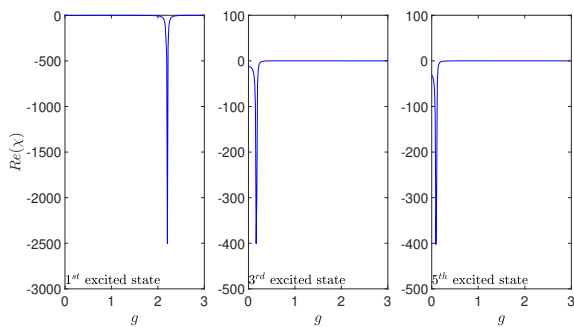


FIG. 9: The fidelity susceptibility as a function of the coupling strength g for the 1st excited state (left panel), the 3rd excited state (middle panel) and the 5th excited state (right panel) at $\Delta = 1.0$.

IV. SUMMARY AND DISCUSSIONS

In this work, we have compactly derived the G -function for the non-Hermitian QRM and tpQRM using the Bogoliubov operators approach, whose zeros determine the energy spectrum. Specifically, in the \mathcal{PT} regime, the G -function is defined in real variable space. This enables the detection of EPs when both the G -function and its derivative with respect to E are zero. Through the G -function, we have confirmed the complex-conjugate spectra of non-Hermitian systems with \mathcal{PT} symmetry, and in the \mathcal{PT} -broken regime, the \mathcal{PT} operator transforms one eigenstate to its conjugate counterpart. Numerous EPs are situated within the two nearest-neighbor energy levels, resulting in an infinite number of EPs. With higher energy levels, the EP shrinks to the smaller coupling strength. The fidelity susceptibility goes to negative infinity around the EPs, consistent with the recent observation in other non-Hermitian systems.

Remarkably, the lowest two excited levels with robust real energies in the non-Hermitian tpQRM at $\Delta = 1.0$ exhibit a novel EP. The EP irrelevant to the complex energies may have particular applications in those dissipative systems which can be described by the non-Hermitian theory. The mechanism for the true crossing of real levels within the same parity and the same Bargmann index in the tpQRM is yet to be identified. Further study is needed to clarify this issue.

Finally, we discuss the integrability of the non-Hermitian QRMs, according to Braak's criterion of quantum integrability in the Hermitian QRM [39]. It is stated that if the eigenstates can be uniquely labeled by $f = f_1 + f_2$ quantum numbers, where f_1 and f_2 are the numbers of the discrete (two levels) and continuous (photons) degrees of freedom, the system is integrable. The present two non-Hermitian QRMs also possess the Z_2 symmetry (in each Bargmann space for the tpQRM) and have the same number of the symmetry (conserved energy and parity), similar to the Hermitian QRMs. Even at EPs, two eigenenergies and two eigenvalues coalesce within the same parity, the single eigenstate can be labeled by the conserved energy. Therefore, we may claim that the non-Hermitian QRMs are also integrable.

ACKNOWLEDGMENTS

This work is supported in part by the National Natural Science Foundation of China (Grants No. 11834005 and No. 12305032).

[1] J. Feinberg and A. Zee, Physical Review E **59**, 6433 (1999).

[2] J. Ren, P. Hänggi, and B. Li, Physical Review Letters **104**, 170601 (2010).

- [3] S. Longhi, *Physical Review A* **88**, 062112 (2013).
- [4] T. E. Lee and C.-K. Chan, *Physical Review X* **4**, 041001 (2014).
- [5] X. Gao and W. Thiel, *Physical Review E* **95**, 013308 (2017).
- [6] K. Li and Y. Xu, *Physical Review Letters* **129**, 093001 (2022).
- [7] D. C. Brody, *Journal of Physics A: Mathematical and Theoretical* **47**, 363505 (2014).
- [8] A. Fring and T. Frith, *Physical Review A* **95**, 010102 (2017).
- [9] Y. Ashida, Z. Gong, and M. Ueda, *Advances in Physics* **69**, 249 (2020).
- [10] Y.-C. Tzeng, C.-Y. Ju, G.-Y. Chen, and W.-M. Huang, *Physical Review Research* **3**, 013015 (2021).
- [11] E. Edvardsson and E. Ardonne, *Physical Review B* **106**, 115107 (2022).
- [12] C. M. Bender and S. Boettcher, *Physical Review Letters* **80**, 5243 (1998).
- [13] A. Mostafazadeh, *Journal of Mathematical Physics* **43**, 205 (2002).
- [14] A. Mostafazadeh, *Journal of Mathematical Physics* **43**, 2814 (2002).
- [15] C. M. Bender, *Journal of Physics: Conference Series* **631**, 012002 (2015).
- [16] C. E. Rüter, K. G. Makris, R. El-Ganainy, D. N. Christodoulides, M. Segev, and D. Kip, *Nature Physics* **6**, 192 (2010).
- [17] L. Feng, Z. J. Wong, R.-M. Ma, Y. Wang, and X. Zhang, *Science* **346**, 972 (2014).
- [18] V. V. Konotop, J. Yang, and D. A. Zezyulin, *Reviews of Modern Physics* **88**, 035002 (2016).
- [19] R. El-Ganainy, K. G. Makris, M. Khajavikhan, Z. H. Musslimani, S. Rotter, and D. N. Christodoulides, *Nature Physics* **14**, 11 (2018).
- [20] W.-C. Wang, Y.-L. Zhou, H.-L. Zhang, J. Zhang, M.-C. Zhang, Y. Xie, C.-W. Wu, T. Chen, B.-Q. Ou, W. Wu, H. Jing, and P.-X. Chen, *Physical Review A* **103**, L020201 (2021).
- [21] M.-A. Miri and A. Alù, *Science* **363**, eaar7709 (2019).
- [22] t. K. Özdemir, S. Rotter, F. Nori, and L. Yang, *Nature Materials* **18**, 783 (2019).
- [23] A. Li, H. Wei, M. Cotrufo, W. Chen, S. Mann, X. Ni, B. Xu, J. Chen, J. Wang, S. Fan, C.-W. Qiu, A. Alù, and L. Chen, *Nature Nanotechnology* 10.1038/s41565-023-01408-0 (2023).
- [24] I. I. Rabi, *Physical Review* **49**, 324 (1936).
- [25] M. O. Scully and M. S. Zubairy, *Quantum Optics* (Cambridge University Press, 1997).
- [26] D. Leibfried, R. Blatt, C. Monroe, and D. Wineland, *Reviews of Modern Physics* **75**, 281 (2003).
- [27] D. Englund, A. Faraon, I. Fushman, N. Stoltz, P. Petroff, and J. Vučković, *Nature* **450**, 857 (2007).
- [28] K. Hennessy, A. Badolato, M. Winger, D. Gerace, M. Atatüre, S. Gulde, S. Fält, E. L. Hu, and A. Imamoglu, *Nature* **445**, 896 (2007).
- [29] T. Niemczyk, F. Deppe, H. Huebl, E. P. Menzel, F. Hocke, M. J. Schwarz, J. J. Garcia-Ripoll, D. Zueco, T. Hümmer, E. Solano, A. Marx, and R. Gross, *Nature Physics* **6**, 772 (2010).
- [30] L. B. Gluhovik, Q. Chen, M. T. Batchelor, and E. Solano, *Journal of Physics A: Mathematical and Theoretical* **49**, 300301 (2016).
- [31] P. Forn-Díaz, J. J. García-Ripoll, B. Peropadre, J.-L. Orgiazzi, M. A. Yurtalan, R. Belyansky, C. M. Wilson, and A. Lupascu, *Nature Physics* **13**, 39 (2017).
- [32] P. Forn-Díaz, L. Lamata, E. Rico, J. Kono, and E. Solano, *Reviews of Modern Physics* **91**, 025005 (2019).
- [33] P. Bertet, S. Osnaghi, P. Milman, A. Auffeves, P. Maioli, M. Brune, J. M. Raimond, and S. Haroche, *Physical Review Letters* **88**, 143601 (2002).
- [34] S. Stuffer, P. Machnikowski, P. Ester, M. Bichler, V. M. Axt, T. Kuhn, and A. Zrenner, *Physical Review B* **73**, 125304 (2006).
- [35] E. Del Valle, S. Zippilli, F. P. Laussy, A. Gonzalez-Tudela, G. Morigi, and C. Tejedor, *Physical Review B* **81**, 035302 (2010).
- [36] S. Felicetti, J. S. Pedernales, I. L. Egusquiza, G. Romero, L. Lamata, D. Braak, and E. Solano, *Physical Review A* **92**, 033817 (2015).
- [37] L. Cong, X.-M. Sun, M. Liu, Z.-J. Ying, and H.-G. Luo, *Physical Review A* **99**, 013815 (2019).
- [38] Z.-J. Ying, *Physical Review A* **103**, 063701 (2021).
- [39] D. Braak, *Physical Review Letters* **107**, 100401 (2011).
- [40] Q.-H. Chen, C. Wang, S. He, T. Liu, and K.-L. Wang, *Physical Review A* **86**, 023822 (2012).
- [41] L. Duan, Y.-F. Xie, D. Braak, and Q.-H. Chen, *Journal of Physics A: Mathematical and Theoretical* **49**, 464002 (2016).
- [42] Q. Xie, H. Zhong, M. T. Batchelor, and C. Lee, *Journal of Physics A: Mathematical and Theoretical* **50**, 113001 (2017).
- [43] J. Li and Q.-H. Chen, *Journal of Physics A: Mathematical and Theoretical* **53**, 315301 (2020).
- [44] Y.-F. Xie and Q.-H. Chen, *Physical Review Research* **3**, 033057 (2021).
- [45] D. Braak, *Annalen der Physik* **535**, 2200519 (2023).
- [46] T. E. Lee and Y. N. Joglekar, *Physical Review A* **92**, 042103 (2015).
- [47] Q. Xie, S. Rong, and X. Liu, *Physical Review A* **98**, 052122 (2018).
- [48] X. Lu, H. Li, J.-K. Shi, L.-B. Fan, V. Mangazeev, Z.-M. Li, and M. T. Batchelor, *Physical Review A* **108**, 053712 (2023).